Acoustic emission in dynamic compression and its relevance to tribology

Doraiswami Ravi and A. Sethuramiah*

In the present work an acoustic emission (AE) technique is used to detect the initiation and propagation of short cracks in compressive cyclic loading. A mild steel surface was subjected to cyclic compressive stress of 100 cycles s^{-1} by an electromagnetic exciter system. The compressive load applied was in the range of 2.5 to 25 N in each cycle. The stressing was done with an En31 steel ball in the presence of turbine oil. Acoustic emission was detected by placing an AE sensor 1.5 cm away from the point of contact of ball and plate. The surface damage was observed to be negligible until 10^4 cycles. Microcrack nucleation and/or growth were inferred until 0.6×10^5 cycles. Thereafter the acoustic emission activity decreased, suggesting possible arrest mechanisms were operating. The emission activity again became very significant beyond 6.0×10^5 cycles, which may be due to possible subsurface crack growth. This information is related to previous one-pass sliding experiments.

Keywords: *acoustic emission, microcracks, ringdown counts, peak amplitude*

Introduction

Acoustic emission (AE) is generated by fundamental mechanical processes. Its detection and analysis have been extensively used as an effective tool to understand nucleation and propagation of cracks in materials[1–3]. More recently AE techniques have been applied to tribological problems of friction and wear in sliding/rolling contacts. Attempts have been made to understand variation in friction, wear behaviour and lubricant influence through monitoring of AE in real time[5–10]. Such studies can be useful in distinguishing between different wear mechanisms and lubricants in sliding contacts. These studies rely on the global emission from a large number of varying contact events and are statistical in nature. It may be more useful to utilize AE to study the events that lead to surface damage. In the present work AE has been studied under cyclic compressive stressing. It is felt such a study will help in understanding the damage processes in tribological contact. This is linked to previous work[11,12] in which fatigue wear was modelled on the basis of one-pass sliding of pre-stressed material.

Industrial Tribology, Machine Dynamics and Maintenance Engineering Center, Indian Institute of Technology, New Delhi 110016, India.
Received 31 January 1994; revised 30 August 1994; accepted 26 October 1994
* *Author to whom correspondence should be addressed*

Experimental

An investigation was carried out on a slow speed reciprocating test machine[11]. The investigation was done with dynamic compression only and no sliding test was done. A schematic diagram of the machine is shown in Fig 1. The cyclic loading was done by an electromagnetic exciter. A schematic diagram of the system is shown in Fig 2. The strain is measured by four strain gauges connected to form a Wheatstone bridge on the circular ring made of spring steel. The strain signal is amplified through a carrier amplifier and displayed on a chart recorder. The strain gauge was calibrated with a static load over the range of 9.8–98 N and a good linear relationship was observed. To apply cyclic loads, the ring was first loaded to a predetermined level by screwing the nut B to the level needed and then locking it with nut C. To impart a dynamic load, an electromagnetic exciter operated with 230 V a.c. supply via an RC-type oscillator with

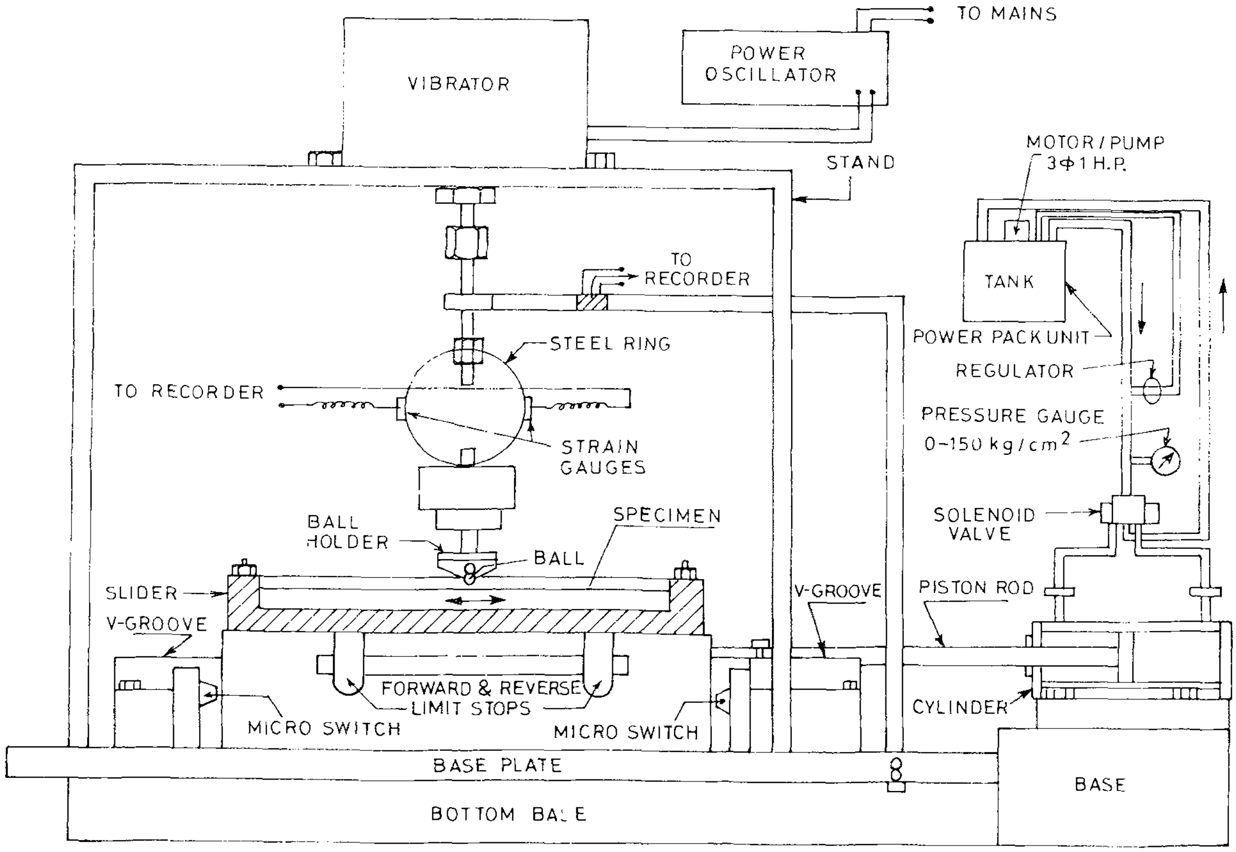

Fig 1 Slow speed reciprocating machine

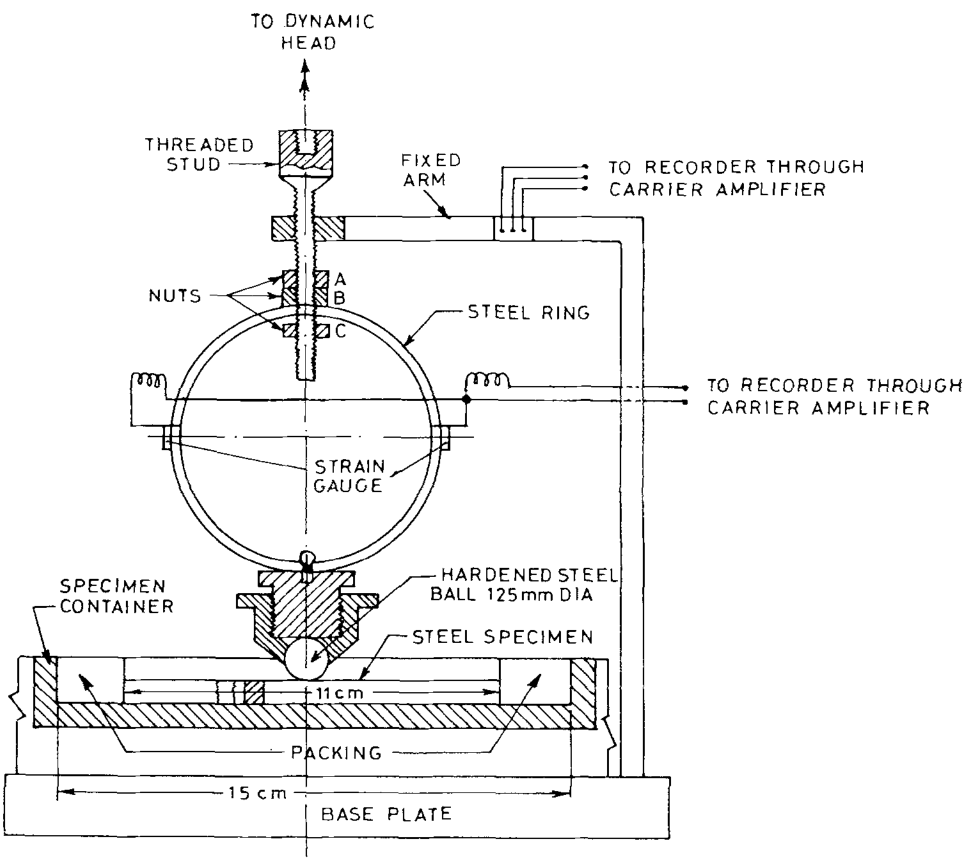

Fig 2 Set-up for cyclic loading

built-in power amplifier was used. The frequency and amplitude can be controlled with the time period setting knob and amperage setting knob respectively. For the present work a frequency of 100 cycles s^{-1} was used. The cyclic load was applied by coupling the threaded stud and then vibrating the system. The setting was adjusted so that the load varied between 2.5 and 25 N in one cycle. The average initial hertzian stress at 25 N was 1.25 Y, where Y is the yield stress. As the stress cycles increase the diameter slowly increases and the overall stress decreases, as discussed in detail in our earlier communication[12]. During cyclic loading, the signal from the carrier amplifier was periodically checked with a cathode ray oscilloscope and it was ensured that the frequency and load range were accurately maintained throughout the cyclic loading.

An En 31 steel ball of diameter 0.01252 m was used as the upper specimen. A mild steel (MS) plate of dimensions 0.10 m × 0.02 m × 0.005 m was used as the lower specimen. The MS specimen was prepared from commercially available plate. The samples were immersed in turbine oil and stored in a desiccator. After cleaning both the upper and lower specimens ultrasonically with benzene and drying, the specimens were positioned for stressing in the presence of lubricating oil. This was accomplished by adding a drop of turbine oil in the contact zone before starting the experiment.

Acoustic emission was detected by positioning a piezoelectric transducer (AC 275 from AET Corp.), close to the point of contact on the lower specimen at a distance of 1.5 cm away from the point of contact. The transducer with a resonant frequency of 275 kHz was followed by a pre-amplifier (AET FL 25) with appropriate plug-in filter. The signal was post amplified before being analysed by the AET 5000 processing system.

The data was collected after setting the clock periods of event duration to 1000 ns, the clock periods of rise time to 250 ns, the threshold setting to 1 V automatic and the preamplifier gain to 60 dB.

Results and discussion

Data analysis was made on the basis of information obtained with regard to distribution of events by ringdown counts and peak amplitudes in each 10 min interval upto 1 h 50 min which corresponds to 6.6 × 10^5 cycles. The information is plotted in Figs 3 to 10. Two intervals of 2.4 to 3.0 × 10^5 cycles and 5.4 to 6.0 × 10^5 were not plotted.

Figure 3(a) gives a plot of the distribution of events by ringdown counts while Fig 3(b) gives information on the distribution of events by peak amplitude for the first 10 min which represents 0 to 0.6 × 10^5 cycles. This zone which involves elasto-plastic deformations at the asperity and hertzian contact level resulted in a broad spectrum of RDC and peak amplitudes. The

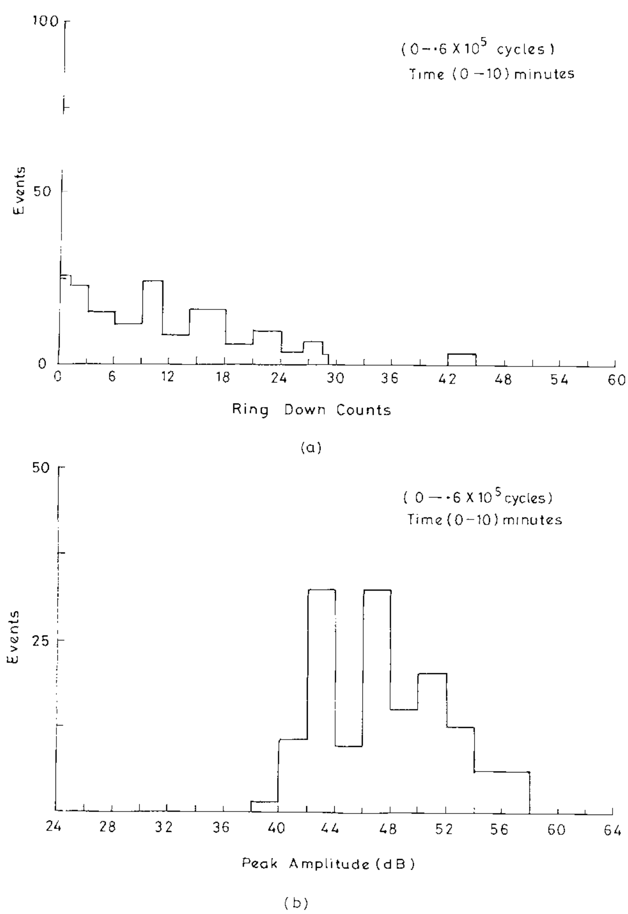

Fig 3 (a) Distribution of events by ring down counts; (b) distribution of events by peak amplitude (dB)

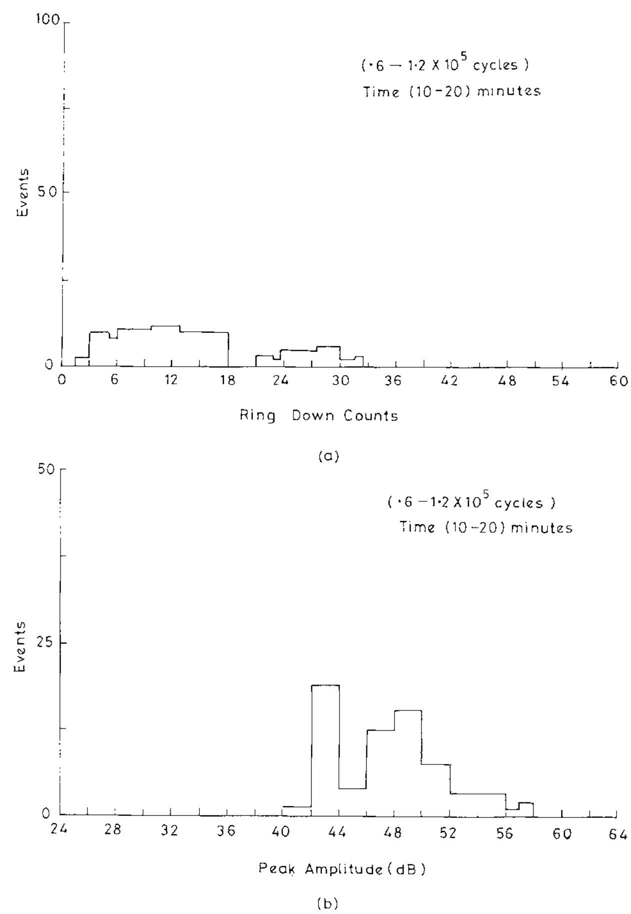

Fig 4 (a) Distribution of events by ring down counts; (b) distribution of events by peak amplitude (dB)

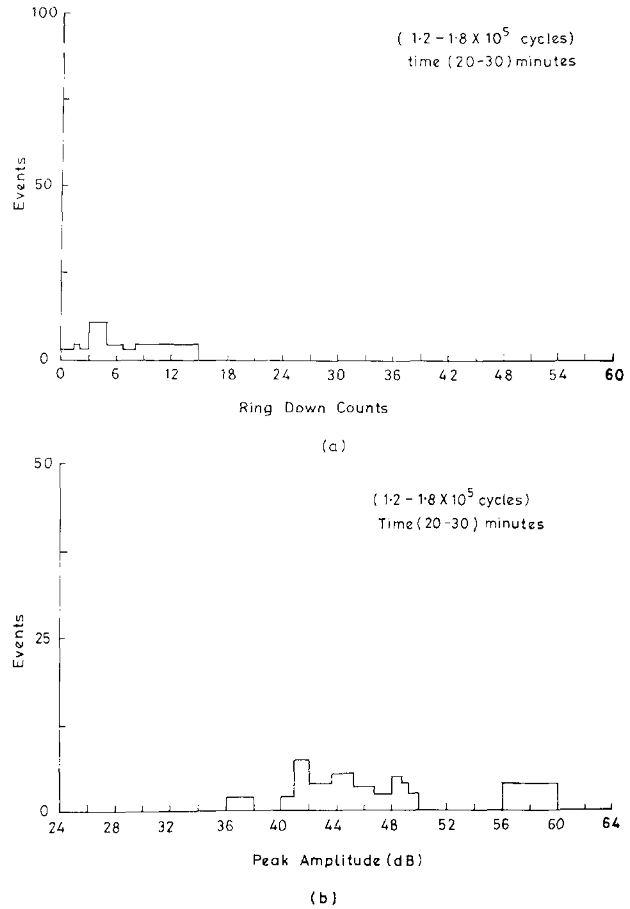

Fig 5 *(a) Distribution of events by ring down counts; (b) distribution of events by peak amplitude (dB)*

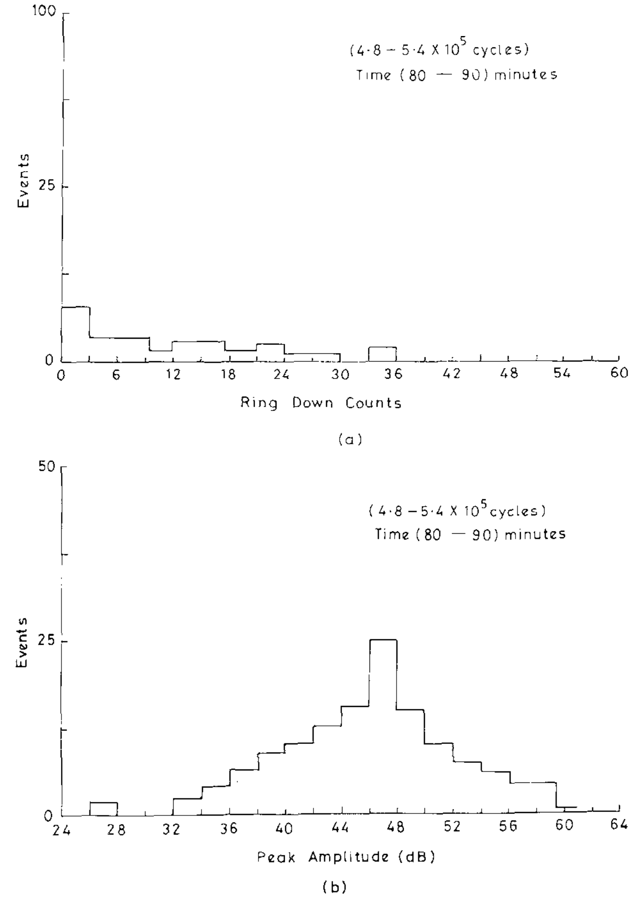

Fig 6 *(a) Distribution of events by ring down counts; (b) distribution of events by peak amplitude (dB)*

deformation in this zone involves elasto-plastic to significantly elastic deformations at the asperities. The significant number of sharp events (those with low RDC) indicates that crack nucleation and/or growth process have already set in. The peak amplitudes in the 42–48 dB range are more prominent.

In the 10–20 min range of 0.6 to 1.2×10^5 cycles, Fig 4, the number of events decreased while the prominent peak amplitude range was still 42–48 dB. This figure is indicative of decreasing acoustic emission and is probably related to the behaviour of short cracks which can undergo arrest. Figure 5 representing the next range of 1.2 to 1.8×10^5 cycles clearly shows a drastic decrease in events, indicating arrest mechanisms were operating in this zone. The situation continues up to 4.8×10^5 cycles.

The situation then undergoes a transition to an increased number of events with major peak amplitudes in the 44–48 dB range as shown in Fig 6 for 4.8–5.4×10^5 cycles. This transition can mean a beginning of crack growth into the subsurface.

The next figure, Fig 7 gives information in the 6.0 to 6.6×10^5 cycle range, where a sudden significant increase in AE is observed as evidenced by the large number of sharp events. It is interesting that the prominent peak amplitude range is 42–52 dB and is similar to the previous cases. This sudden increase in activity may be due to crack propagation into the subsurface.

The above analysis is based on the assumption that discrete high amplitude emissions are essentially due to nucleation and growth of cracks. Throughout there is also cyclic deformation. It is known[13] that emissions from cyclic elastic deformation tend to be continuous and of low amplitude. They are likely to be below the threshold selected and hence the assignment of discrete, high amplitude emissions to crack related events is justified.

The above analysis may be now summarized. Surface defect generation and microcrack growth starts in the first ten minutes which amounts to 0.6×10^5 cycles. The contact then undergoes a situation of progressive arrest of microcrack growth which exists until 4.8×10^5 cycles. Beyond this the growth starts again and becomes drastic in the 6.0 to 6.6×10^5 cycle range. This situation most probably represents crack growth into the subsurface. It is of interest to compare the behaviour observed above with one-pass sliding tests done earlier[12]. In these tests mild steel pre-stressed to 10^4, 10^5 and 10^6 cycles with the same stress range as in present investigation was subjected to one-pass sliding and material removal was compared at different normal passage loads and the corresponding surface stresses. The average normal stress during cyclic stressing up to 10^6 cycles ranged from $2.7Y$ to $0.83Y$, due to growth in the contact spot area. With the 10^4 cycle stressed material no wear occurred. The behaviour with other stress cycles in one-pass sliding is compared in Tables 4 and 5 and Fig 6 (a), (c) in

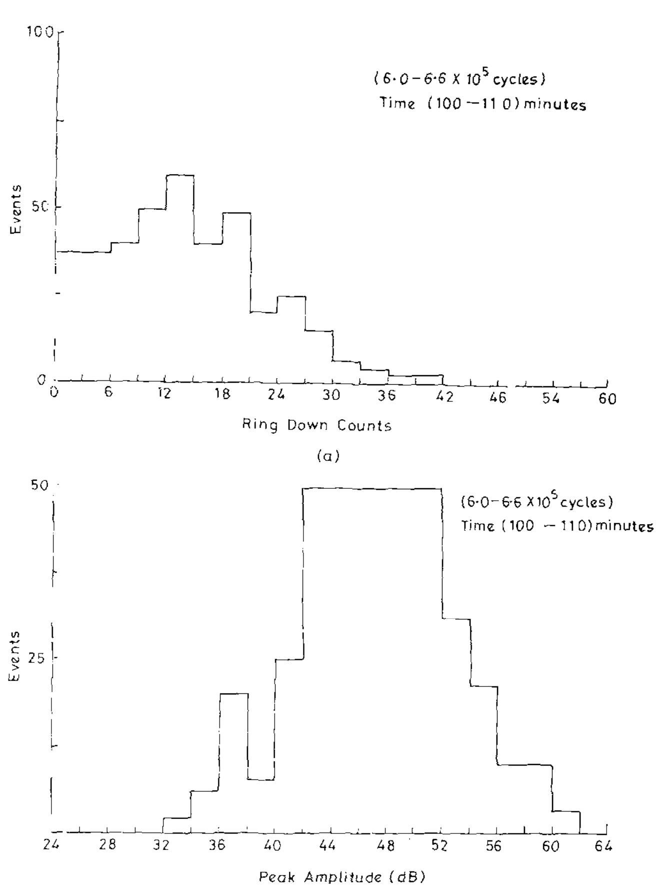

Fig 7 *(a) Distribution of events by ring down counts; (b) distribution of events by peak amplitude (dB)*

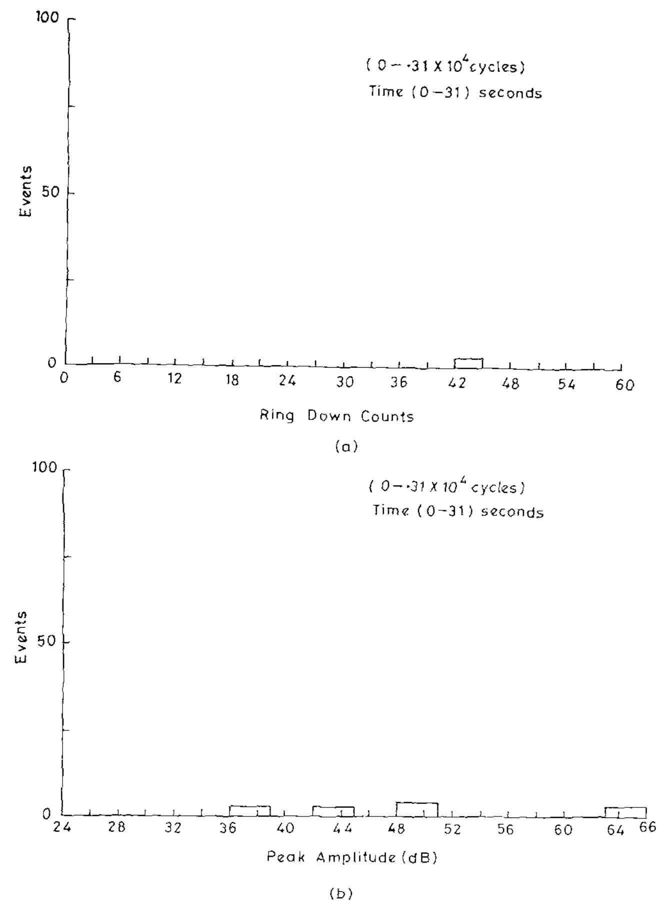

Fig 8 *(a) Distribution of events by ring down counts; (b) distribution of events by peak amplitude (dB)*

our earlier paper[12]. From this information it may be noted that the wear rate with 10^6 cycles spot is 2–4 times higher than 10^5 cycles spot. Also the wear rate increased more steeply with stress in the case of 10^6 cycle spot in comparison to 10^5 cycle spot. It is logical to expect increased removal in sliding wear if the surface/sub-surface damage is higher. Hence this information suggests increased and deeper damage at 10^6 cycles and this is confirmed by the AE investigation discussed above.

No wear was observed with the 10^4 cycle spot. The emission observed up to 0.74×10^4 cycles is shown in Figs 8 and 9. It is remarkable to observe that in the very early stages the surface damage is negligible. Hence the removal in one-pass sliding is expected to be negligible as has been observed in our earlier work.

The experiment was repeated twice and the behaviour observed was similar. As an example the behaviour observed in the range $0–0.88 \times 10^4$ cycles in one of the repeated experiments is given in Fig 10. When this behaviour is compared with Fig 8 discussed earlier the similarity is evident.

The nature of damage observed at each level of stressing can be shown by a detailed study of surface and subsurface. Some information on surfaces is available from previous work[11,12], where photomicrographs of worn and unworn surfaces are compared. The subsurface has not been investigated. We hope to conduct these studies in the future.

Conclusion

Analysis of AE in dynamic compressive stressing in the load range of 2.5–25 N and a frequency of 100 cycles s^{-1} has shown that significant activity occurs beyond 10^4 cycles, which is considered to be due to nucleation and propagation of microcracks. The activity reduces during 1.2×10^5 cycles to 4.8×10^5, which may be due to arrest mechanisms. The activity becomes major beyond 4.8×10^5, probably due to subsurface crack growth. This information could be related to our earlier tribological study with one-pass sliding.

References

1. **Pollock A.A.** Stress-wave emission in NDT. *Nondestr. Testing. 1969*, **August**, *178–182*
2. **Dukes R. and Culpan A.E.** Acoustic emission: its techniques and applications. *IEE Proc. 1948*, **131**, *241–251*
3. **Scruby S.C.** An introduction to acoustic emission. Report AERE.R12139, *National NDT Centre, Material Physics and Metallurgy Division, Harwell Laboratory, February, 1986. 1–15*
4. **Pollock A.A.** Acoustic emission amplitude distributions. *Intern. Adv. Nondestr. Testing, 1981*, **7**, *215–239*
5. **Klamecki B.E. and Hanchi J.** Wear process description based on acoustic emission. *J. Tribol. 1990*, **112**, *469–476*
6. **Sarychev G.A. and Shchavelin V.M.** Acoustic emission method for research and control of friction pairs. *Tribol. Intern. 1991*, **24**, *11–16*
7. **Bones R.J., McBride S.L. and Sobczyk M.** Wear studies using acoustic emission techniques. *Tribol. Intern. 1990*, **23**, *291–295*

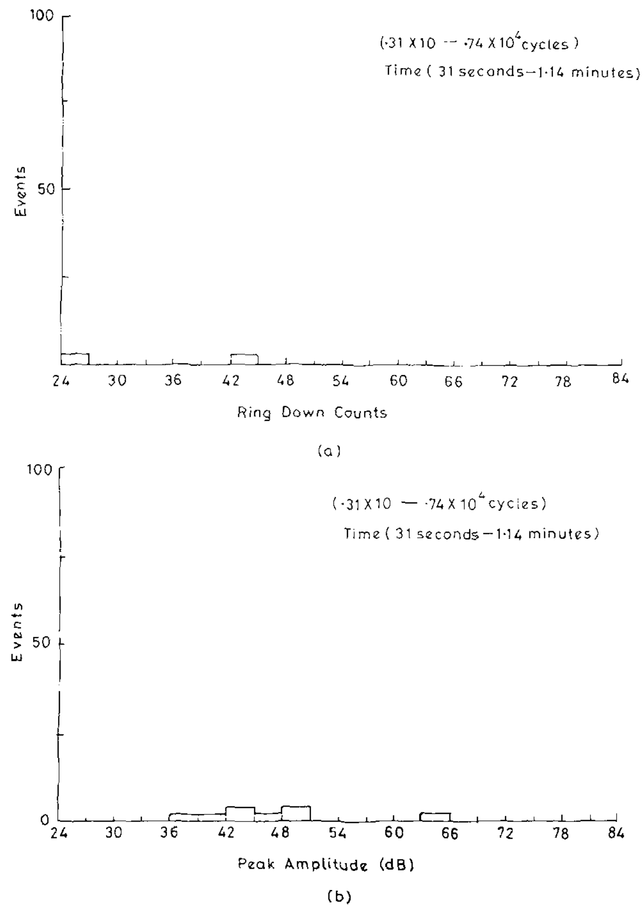

Fig 9 (a) Distribution of events by ring down counts; (b) distribution of events by peak amplitude (dB)

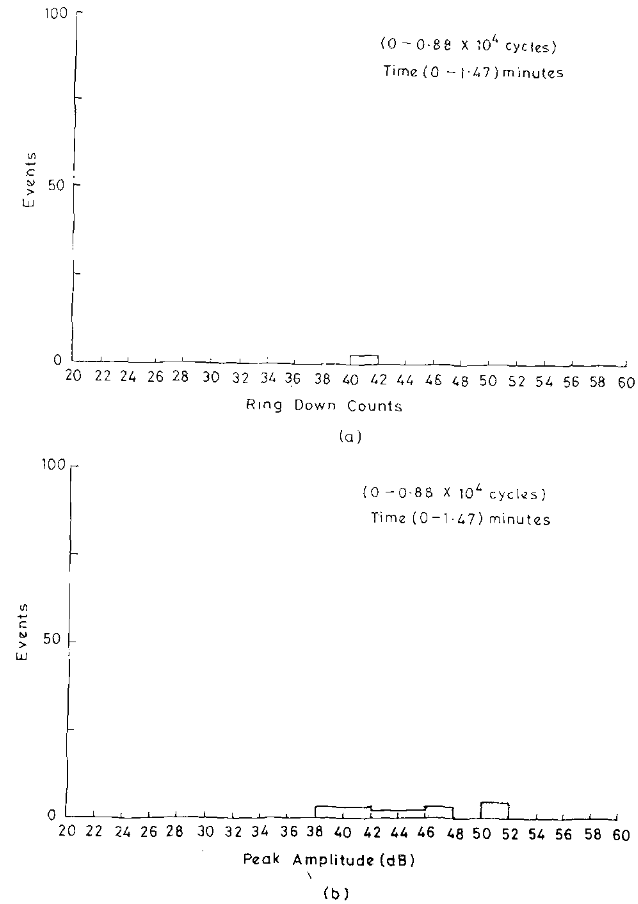

Fig 10 (a) Distribution of events by ring down counts; (b) distribution of events by peak amplitude (dB)

8. **Bones R.J. and McBride S.L.** Adhesive wear studies using acoustic emission techniques. International Conference on Wear of Materials, *Orlando, Florida – US, 1991, ASME Vol I, 425–432*

9. **Lingard S. and Ng K.K.** An investigation of acoustic emission in sliding friction and wear of metals. *Wear*, 1988, **75**, *367–379*

10. **Kannatey-Asibu E., Jr. and Dornfeld D.A.** A study of tool wear using statistical analysis of metal-cutting acoustic emission. *Wear, 1981*, **76**, *247–261*

11. **Karmakar S. and Sethuramiah A.** Response of dynamically stressed material in sliding. *Wear, 1991*, **151**, *269–278*

12. **Karmakar S., Rao U.R.K. and Sethuramiah A.** Characterization of sliding wear in dynamically stressed material. *Wear, 1993*, **162–164**, 1081–1090.

13. **Maslov I.I. and Gradov O.M.** Fracture energy analysis via acoustic emission. *Intern. J. Fatigue, 1986*, **8**, *67–71*